IV. Conclusion

This paper has examined the errors and their impact on the performance of a future-trajectory-based CCWS. This paper follows a statistical approach to characterize the prediction error, incorporate the communication-induced error, and then determine the probability of trajectory conflicts and the quality of the detection performance. Results with test data verify the Kalman-filter-based error statistics estimation and the statistical collision detection. Effects of communication reliability are also examined, and the system demonstrates the potentials of tolerating communication losses and delays.

References

[1] P. Varaiya, "Smart cars on smart roads: Problems of control," *IEEE Trans. Autom. Control*, vol. 38, no. 2, pp. 195–207, Feb. 1993.

[2] S. Kato, S. Tsugawa, K. Tokuda, T. Matsui, and H. Fujii, "Vehicle control algorithms for cooperative driving with automated vehicles and inter-vehicle communications," *IEEE Trans. Intell. Transp. Syst.*, vol. 3, no. 3, pp. 155–160, Sep. 2002.

[3] D. Reichardt, M. Miglietta, L. Moretti, P. Morsink, and W. Schulz, "CarTALK 2000: Safe and comfortable driving based upon inter-vehicle-communication," in *Proc. IEEE Intell. Veh. Symp.*, Versailles, France, Jun. 2002, pp. 545–550.

[4] A. R. Girard, J. B. de Sousa, J. A. Misener, and J. K. Hedrick, "A control architecture for integrated cooperative cruise control and collision warning systems," in *Proc. 40th IEEE Conf. Decision Control*, Orlando, FL, 2001, pp. 1491–1496.

[5] M. Tamura, S. Takahashi, S. Yasuhara, M. Kojima, and K. Minegishi, "Development of intersection safety support systems using vehicle-to-vehicle communication," in *Proc. 12th ITS World Congr.*, San Francisco, CA, 2005.

[6] J. Misener, R. Sengupta, and K. Krishnan, "Cooperative collision warning: Enabling crash avoidance with wireless technology," in *Proc. 12th ITS World Congr.*, San Francisco, CA, 2005.

[7] H.-S. Tan and J. Huang, "DGPS-based vehicle-to-vehicle cooperative collision warning: Engineering feasibility viewpoints," *IEEE Trans. Intell. Transp. Syst.*, vol. 7, no. 4, pp. 415–428, Dec. 2006.

[8] J. Huang and H.-S. Tan, "A low-order DGPS-based vehicle positioning system under urban environment," *IEEE/ASME Trans. Mechatron.*, vol. 11, no. 5, pp. 567–575, Oct. 2006.

[9] B. Fan and H. Krishnan, "Reliability analysis of DSRC wireless communication for vehicle safety applications," in *Proc. IEEE Conf. Intell. Transp. Syst.*, Toronto, ON, Canada, Sep. 2006, pp. 355–362.

IMM-Based Lane-Change Prediction in Highways With Low-Cost GPS/INS

Rafael Toledo-Moreo, *Member, IEEE*, and Miguel A. Zamora-Izquierdo

***Abstract*—The prediction of lane changes has been proven to be useful for collision avoidance support in road vehicles. This paper proposes an interactive multiple model (IMM)-based method for predicting lane changes in highways. The sensor unit consists of a set of low-cost Global Positioning System/inertial measurement unit (GPS/IMU) sensors and an odometry captor for collecting velocity measurements. Extended Kalman filters (EKFs) running in parallel and integrated by an IMM-based algorithm provide positioning and maneuver predictions to the user. The maneuver states Change Lane (CL) and Keep Lane (KL) are defined by two models that describe different dynamics. Different model sets have been studied to meet the needs of the IMM-based algorithm. Real trials in highway scenarios show the capability of the system to predict lane changes in straight and curved road stretches with very short latency times.**

***Index Terms*—Inertial sensors, interactive multiple model (IMM), lane change, maneuver prediction.**

I. Introduction

The problem of collisions on highways may be addressed from different points of view. In the current literature, three different paradigms can be found for collision-avoidance support: Alert panels and messages coming from the traffic authorities to warn the drivers in the area of interest, solutions based on an intelligent vehicle capable of dealing with unfriendly and changing environments, and collaborative systems in which all the vehicles involved in the scene play a role. In the last two cases, but particularly the latter, a timely lane-change warning system can be very useful while requiring high penetration rate and, therefore, low cost.

In this paper, a low-cost system for lane prediction based on Global Positioning System (GPS) and Inertial Navigation System (INS) sensors is presented. The performance of the INS sensors strongly depends on the technology used and the unit price. Since market considerations are taken into account in this research, only low-cost microelectromechanical systems (MEMS) devices are considered in the onboard equipment (OBE) of the vehicle. GPS and INS data, along with odometry values, are fused in a interactive multimodel (IMM)-based filter with individual extended Kalman filters (EKFs) for the maneuver states *Change Lane* (CL) and *Keep Lane* (KL).

Over the past few years, IMM-based methods have been used to increase the accuracy of navigation systems in aerial and road navigation. In our research, its capability to model the vehicle behavior with

Manuscript received September 4, 2007; revised February 5, 2008 and July 1, 2008. First published February 3, 2009; current version published February 27, 2009. This work was supported by the Spanish Ministerio de Fomento under Grant FOM/2454/2007. This work has been carried out inside the Intelligent Systems Group, University of Murcia, awarded as an excellence researching group in frames of the Spanish Plan de Ciencia y Tecnología de la Regíon de Murcia. The Associate Editor for this paper was Y. Wang.

R. Toledo-Moreo is with the Department of Electronics and Computer Technology, Technical University of Cartagena, 30202 Cartagena, Spain (e-mail: rafael.toledo@upct.es).

M. A. Zamora-Izquierdo is with the Department of Information and Communication Engineering, University of Murcia, 30071 Murcia, Spain (e-mail: mzamora@um.es).

Color versions of one or more of the figures in this paper are available online at http://ieeexplore.ieee.org.

Digital Object Identifier 10.1109/TITS.2008.2011691

different dynamics has been found to be useful to obtain uninterrupted more precise positioning and integrity values [8]. In this paper, we analyze its suitability to distinguish between two maneuver states, comparing different model sets dedicated to represent the nature of *CL* and *KL* maneuvers. A first approach where highway trajectories are assumed to have low-curvature values was tested by obtaining positive results where this assumption was found feasible. However, in cases of more curved trajectories, the results obtained by this model were found to be poor. For this reason, information of the horizontal alignment of the road was included in the filter, obtaining consistent results. Digital maps are used to collect this road information, and an algorithm to estimate the road curvature has been applied.

The rest of this paper is organized as follows. First, the most relevant related work in this issue is discussed. Next, multiple model-filtering techniques and vehicle models applied in this paper will be presented. In Section IV, the OBE of the vehicle and the results of experimental trials with real data are shown. The main conclusions are finally discussed.

II. Related Work

Lane-change collision-avoidance systems are designed to prevent crashes in lane-change maneuvers when the vehicle enters a potentially conflictive area for the surrounding vehicles on the sides and behind [1]. Lane-change prediction is approached in the literature from many different points of view, most of them based on vision systems [2], [19], [20]. In [2], the authors make a comparison of previous research that distinguishes between driver intent inference and trajectory prediction.

The method proposed in this paper predicts lane changes based on the vehicle dynamics, being independent of the visibility, weather conditions, or blockages of the GPS signals. The idea of using multiple models for representing different vehicle dynamics has more extensively been used in aerial navigation [10]. Over the past few years, several authors applied multiple model-based methods to the road transportation field, particularly for object tracking [3], [4], [15] and navigation purposes [8], [13], [14].

In this case, IMM focuses on maneuver predictions by meeting the searched vehicle dynamics. To represent the different maneuver states of a vehicle along the road, most of the authors use constant velocity (CV), constant acceleration (CA), and stationary (S) models [14], [15]. In our case, we concentrate on lateral movements.

According to our models, the road shape information must be employed to distinguish between lateral maneuvers. A good example of the actual capabilities of maps for this purpose can be found in [16]. The road shape can be modeled in different manners, such as segments of straight lines, arcs, and clothoids. In the current literature, models with high success consider the road segment as a clothoid curve [17], [18]. Moreover, this idea agrees with the way roads are constructed [9]. Nevertheless, a model that exactly represents a clothoid curve is very complicated, and approximations like the one presented in this paper are usually employed [11]. Regarding road curvature estimation based on maps, a common approach is the use of piecewise polynomials (spline) that are fitted to the road trajectory [22]–[24].

III. Multiple Model Filtering

The basic idea of using multiple models is based on the fact that a vehicle performs very different maneuvers, depending on the scenario features. For a road vehicle, typical maneuvers in highways differ from those usual in city environments. Thus, a single vehicle model can hardly represent all the possible maneuvers, and the use of multiple models, which represent different maneuver states and running in parallel, is advisable. There are many ways to combine multiple models in just one filter [5]. The model presented in the next section has been found appropriate for our purposes, according to the results achieved in the tests.

A. Interactive Multiple Model

In the IMM approach, the manner in which the state estimates from the individual filters are combined depends on a Markovian model for the transition between maneuver states. The IMM method can be described according to four different parts.

1) Interaction: In this section, individual filters are mixed according to the predicted model probabilities. The predicted model probability is given by the model probability in the previous cycle $\mu^{(j)}_{k-1|k-1}$ and the probability that a transition from state j to state i occurs π_{ji}, i.e.,

$$\mu^{(i)}_{k|k-1} = \sum_j \pi_{ji}\mu^{(j)}_{k-1|k-1} \tag{1}$$

being the conditional model probability, given the object is in state i that the transition occurred from state j

$$\mu^{(j|i)}_{k-1|k-1} = \frac{\pi_{ji}\mu^{(j)}_{k-1|k-1}}{\mu^{(i)}_{k|k-1}} \tag{2}$$

and the mixing of the state estimates $\hat{\mathbf{x}}^{(j)}_{k-1|k-1}$ and covariances $\mathbf{P}^{(j)}_{k-1|k-1}$ as

$$\bar{\mathbf{x}}^{(i)}_{k-1|k-1} = \sum_j \mu^{(j|i)}_{k-1|k-1}\hat{\mathbf{x}}^{(j)}_{k-1|k-1} \tag{3}$$

$$\begin{aligned}\bar{\mathbf{P}}^{(i)}_{k-1|k-1} = \sum_j \mu^{(j|i)}_{k-1|k-1} \\ \times \left[\mathbf{P}^{(j)}_{k-1|k-1} + \left(\bar{\mathbf{x}}^{(i)}_{k-1|k-1} - \hat{\mathbf{x}}^{(j)}_{k-1|k-1}\right)\right. \\ \left. \times \left(\bar{\mathbf{x}}^{(i)}_{k-1|k-1} - \hat{\mathbf{x}}^{(j)}_{k-1|k-1}\right)'\right].\end{aligned} \tag{4}$$

The probabilities π_{ji} that a transition occurred from state j to state i are calculated according to a Markovian process, as described in [10], and will depend on the statistics of real traffic situations related to the mean sojourn times and the sampling interval. In our tests, the next values were fixed: $\pi_{11} = 0.981$, $\pi_{12} = 0.019$, $\pi_{21} = 0.011$, and $\pi_{22} = 0.989$.

2) Model Individual Filtering: Now, individual filters predict and update their state and covariance by using their kinematical assumptions. The predicted state estimates $\hat{\mathbf{x}}^{(i)}_{k|k-1}$ and covariances $\mathbf{P}^{(i)}_{k|k-1}$ will be calculated by using a loosely coupled EKF, as described in [5]. The kinematical models used will be presented in the next sections. Innovations and their covariances are calculated in this phase also following [5].

3) Model Probability Update: In this section, each model probability is updated according to the innovation error. Assuming Gaussian statistics, the likelihood for the observation can be calculated from the innovation vector $\nu^{(i)}_k$ and its covariance $\mathbf{S}^{(i)}_k$ following

$$\Lambda^{(i)}_k = \frac{\exp\left[-(1/2)\left(\nu^{(i)}_k\right)'\left(\mathbf{S}^{(i)}_k\right)^{-1}\nu^{(i)}_k\right]}{\sqrt{\left|2\pi\mathbf{S}^{(i)}_k\right|}} \tag{5}$$

and updating the predicted model probabilities as

$$\mu_{k|k}^{(i)} = \frac{\mu_{k|k-1}^{(i)} \Lambda_k^{(i)}}{\sum_j \mu_{k|k-1}^{j} \Lambda_k^{(j)}}. \quad (6)$$

4) Combination: The combined state $\hat{\mathbf{x}}_{k|k}$ and its covariance $\mathbf{P}_{k|k}$ are now calculated from the weighted state estimates $\hat{\mathbf{x}}_{k|k}^{(i)}$ and covariances $\hat{\mathbf{P}}_{k|k}^{(i)}$ as

$$\hat{\mathbf{x}}_{k|k} = \sum_i \mu_{k|k}^{(i)} \hat{\mathbf{x}}_{k|k}^{(i)} \quad (7)$$

$$\mathbf{P}_{k|k} = \sum_i \mu_{k|k}^{(i)} \left[\mathbf{P}_{k|k}^{(i)} + \left(\hat{\mathbf{x}}_{k|k} - \hat{\mathbf{x}}_{k|k}^{(i)} \right) \left(\hat{\mathbf{x}}_{k|k} - \hat{\mathbf{x}}_{k|k}^{(i)} \right)' \right]. \quad (8)$$

B. Model Sets

To distinguish lane-change maneuvers in highways, different model sets were tested. Among them, those two that presented the most interesting results are presented next. In both cases, the kinematic model proposed is a simplified bicycle model in which the orientations of the acceleration and velocity vectors are assumed to be equal. The results achieved in [6] and [7] and this paper show that this assumption can be done.

1) Model-Set A: The first model-set tested is based on [7]. In this paper, it is considered that the curvatures in highway scenarios are low enough not to influence the trajectory recognition of a lane change. Two maneuver cases are considered.

1) Change Lane (CL/A). The state vector of the CL/A model is $\mathbf{x}_{CL/A} = (x, y, \phi, v, \omega, a)$, which represent the east, north, velocity angle, velocity, yaw rate of turn, and acceleration in the center of mass of the vehicle. The dynamics of this model are described by

$$\dot{\mathbf{x}}_{\mathrm{CL/A}} = [(v + at)\ \cos(\phi)\ (v + at)\ \sin(\phi)\ \omega\ a\ 0\ 0]' + \left[0\ 0\ 0\ 0\ \eta_{\omega_{\mathrm{CL/A}}}\ \eta_{a_{\mathrm{CL/A}}}\right]' \quad (9)$$

where $\eta_{\omega_{\mathrm{CL/A}}}$ and $\eta_{a_{\mathrm{CL/A}}}$ are the random walk terms representing the errors due to the model assumptions of CA and constant yaw rate with values of 0.15 rad/s^2 and 4.0 m/s^3, respectively.

2) Keep Lane (KL/A). The state vector of the KL/A model is the same as in the CL/A model. However, in this case, a constant yaw is assumed between periods, where $\omega = 0$, and the differential equation is

$$\dot{\mathbf{x}}_{\mathrm{KL/A}} = [(v + at)\ \cos(\phi)\ (v + at)\ \sin(\phi)\ 0\ a\ 0\ 0]' + \left[0\ 0\ \eta_{\phi_{\mathrm{KL/A}}}\ 0\ \eta_{\omega_{\mathrm{KL/A}}}\ \eta_{a_{\mathrm{KL/A}}}\right]'. \quad (10)$$

In this case, a new term $\eta_{\phi_{\mathrm{KL/A}}}$ must be considered for errors in the constant yaw assumption, where its value is 0.2 rad/s. In addition, the noise parameters due to ω must be much lower to represent the vehicle dynamics of this case (0.0205 rad/s^2). The observations for the CL/A and KL/A individual filters are GPS east and north values $(x_{\mathrm{gps}}, y_{\mathrm{gps}})$, odometry velocity (v_{odo}), and inertial measurements for angular rate (ω_{ins}) and longitudinal acceleration (a_{ins}). The noise parameters are fixed in the tuning process of the filter, starting from the sensor specifications with final values: $\sigma_{\mathrm{gps}} = 0.6$ m/s, $\sigma_{v_{\mathrm{odo}}} = 0.0198$ m/s^2, $\sigma_{\omega_{\mathrm{ins}}} = 0.01038$ rad/s^2, and $\sigma_{a_{\mathrm{ins}}} = 0.0996$ m/s^3.

2) Model-Set B: For this model set, the value of the curvature of the road is employed. To do that, and taking into account that curvature is not available in current maps, some calculations must be done using road position values (as explained in the next section). In model-set B, the horizontal alignment of the road is described by clothoid curves in which the curvature linearly changes with the traveled distance. In this paper, we do not pay attention on the 3-D aspects of the road, assuming that the vertical motions in highways can be negligible, as compared with those in the horizontal plane.

Since exact clothoid models are very complicated, based on [11], in this paper, we assume that the road shape is describe by $c(s) = c_0 + c_1 s$, where $c(s)$ represents the curvature as a function of the longitudinal distance, and c_0 and c_1 are fitting parameters that are dependent on time. The results obtained in the literature and this paper found favorable this approximation.

1) Change Lane (CL/B). The state vector of the CL/B model is $\mathbf{x}_{\mathrm{CL/B}} = (x, y, \phi, v, \omega, a, c_0, c_1)$, which represent the east, north, velocity angle, velocity, yaw rate of turn, and acceleration in the center of mass of the vehicle, and the two parameters for adjusting the road shape. Based on (9) and the proposed clothoid model, the dynamics of this model are described by

$$\dot{\mathbf{x}}_{\mathrm{CL/B}} = [(v + at)\ \cos(\phi)\ (v + at)\ \sin(\phi)\ \omega\ a\ 0\ 0\ vc_1\ 0]' + \left[0\ 0\ 0\ 0\ \eta_{\omega_{\mathrm{CL/B}}}\ \eta_{a_{\mathrm{CL/B}}}\ \eta_{c_{0\mathrm{CL/B}}}\ \eta_{c_{1\mathrm{CL/B}}}\right]' \quad (11)$$

where $\eta_{\omega_{\mathrm{CL/B}}}$ and $\eta_{a_{\mathrm{CL/B}}}$ are analogous to (9) with values of 0.67 rad/s^2 and 4.0 m/s^3, respectively, and $\eta_{c0_{\mathrm{CL/B}}} = 0.05279$ and $\eta_{c1_{\mathrm{CL/B}}} = 1.2793 \cdot 10^{-4}$ m^{-1} are white noise terms that represent the errors due to model assumptions of the road shape.

2) Keep Lane (KL/B). The state vector of the KL/B model is the same as in the CL/B model. However, in this case, the derivative of the angle of the velocity is assumed to follow the road shape, which results in $\dot{\phi} = c_0 v$ and the complete differential equation

$$\dot{\mathbf{x}}_{\mathrm{KL/B}} = [(v + at)\ \cos(\phi)\ (v + at)\ \sin(\phi)\ c_0 v\ a\ 0\ 0\ vc_1\ 0]' + \left[0\ 0\ 0\ 0\ \eta_{\omega_{\mathrm{KL/B}}}\ \eta_{a_{\mathrm{KL/B}}}\ \eta_{c_{0\mathrm{KL/B}}}\ \eta_{c_{1\mathrm{KL/B}}}\right]'. \quad (12)$$

Analogous to model-set A, the noise parameters of this model can be different from those in CL/B because they are fixed in the tuning process of the filter and resulting in $\eta_{\omega_{\mathrm{KL/B}}} = 0.0205$ rad/s^2, $\eta_{c0_{\mathrm{KL/B}}} = 0.00527$, and $\eta_{c1_{\mathrm{KL/B}}} = 1.2793 \cdot 10^{-5}$ m^{-1}. In the experiments presented in this paper, different tests were used to tune and evaluate the system performance to neglect the influence of particular data sets in the results. The observations for the CL/B and KL/B individual filters are the same as those presented in model-set A, along with the value of the curvature obtained from the digital map $c_{0\mathrm{map}}$ explained in the next section.

3) Curvature Estimation: To obtain the value of the road curvature at a given point of the 2-D representation of the road $p(\mathrm{East}, \mathrm{North})$, several tests have been performed with a cubic natural spline, a smoothing spline, and generic third- and upper order splines in a test-bed circuit. Finally, a variation of the third-order polynomial method with a moving window constituted by the n latest coordinates of interest has been used for its good results, assuming $n = 5$ in these experiments. Due to the use of differential GPS (DGPS) Universal Transverse Mercator (UTM) positions in our custom-made digital map, it is advisable to work with Cartesian coordinates. However, to avoid the inconveniences of global heading of the road in the derivatives of the curvature equation, the points selected within the window are previously locally rotated.

The top graph in Fig. 1 shows the circuit N30 used in our experiments, i.e., a very curved road stretch in the Spanish highway N30 Murcia–Cartagena, the points of which were obtained with a

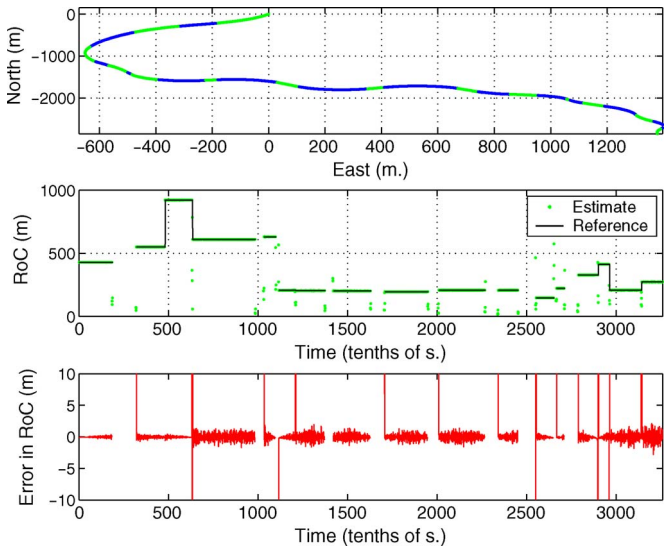

Fig. 1. (Top) Circuit N30 selected for trials with curved roads, consisting of 27 segments and 3269 points that model a piece of the N30 highway from Murcia to Cartagena. (Middle) Radius of curvature (RoC) estimate (dotted green) and reference (solid black) during the N30 circuit. (Bottom) RoC estimated error during the same circuit.

Trimble DGPS Pathfinder Office version 3.0. package with position accuracy of 15 cm. The 27 pieces used to approximate this road have alternatively been colored in blue and green. Below, the estimates of the radius of curvature (dotted green) and the given truth (solid black) during this stretch are compared. The error estimates remain under 2 m, as referred to the assumed truth obtained from the Trimble DGPS custom-made map (bottom image in Fig. 1).

IV. Experimental Results

To avoid the influence of the data sets selected for filter tuning in the system response, different data sets were used for tuning and evaluating the system. The filter output presents different sensitivities for each tuning parameter, being more crucial to those parameters that represent the differences between models. The tuning was made in such a way that the errors lay on the predicted 2σ envelope. Good results can be obtained by following a tuning strategy that was described in [12]. With the appropriate tuning, similar results were obtained in the validation and evaluation processes, which confirms the consistency of the results. Among them, only a few typical situations of overtaking maneuvers on a highway are described in detail in this paper. Apart from lane-change situations, the filter was tested in usual driving situations, showing good performance. Before discussing the results, a brief explanation of the OBE used is given.

A. Onboard Equipment

The hardware architecture of the OBE is based on a standard single-board computer. Serial buses communicate the sensors with the PC via RS232 and controller area network (CAN) bus. BlueTooth, WLAN, and General Packet Radio Service/Universal Mobile Telecommunications System (GPRS/UMTS) links are also available. The inertial measurement units (IMUs) tested are low-cost MEMS-based MT9B by XSens and IMU400 by Xbow. Since it is assumed that the acceleration and velocity vectors are defined by the same angle, only one gyro and one accelerometer are employed. A Trimble DGPS Pathfinder Office version 3.0. was used to evaluate the system performance with a position accuracy of 15 cm. Nevertheless, the Global Navigation Satellite System (GNSS) inputs to the filter were only single uncorrected GPS positions, which results in the map reference being ten times more accurate. Details of the sensor specifications can be found in [8].

TABLE I
Position and Heading Errors of Model-Set A Filters

	KEEP LANE		CHANGE LANE		IMM	
Var.	rms	emax	rms	emax	rms	emax
Pos. (m)	1.12	4.42	1.07	2.13	0.84	2.01
Head. (rad)	0.09	0.29	0.03	0.10	0.03	0.11

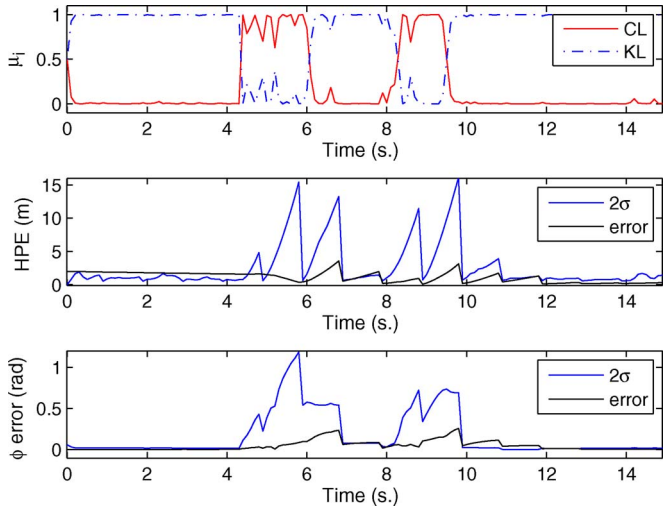

Fig. 2. Test with uninterrupted GPS coverage during a straight stretch. (Top) Model probabilities of the CL (solid red) and KL (dash dotted blue) maneuver states. (Middle and bottom) Horizontal position and heading errors (solid black) and their corresponding 2σ envelopes (solid blue).

B. Results With Model-Set A

Mean values of positioning and heading errors estimated by the individual filters and the IMM-based method over ten tests performed with real data are shown in Table I. As can be seen, the CL filter provides better results for both positioning and heading. The nature of the KL filter impedes the tracking maneuvers with medium or high dynamics. However, the error estimates for heading and position are very different in both cases. While the KL-EKF method underestimates the noise value when lane changes are done, the CL-EKF option provides unrealistic estimates for straight trajectories without lane changes. On the other hand, in the IMM/A case, the RMS value for the positioning error diminishes, as compared with individual single filters, whereas EMAX is close to the CL value. Similar values as those obtained in the CL filter are achieved for heading. Nevertheless, despite the fact that the IMM filter is found to be capable of improving the filter accuracy, the main scope of this paper is not pose estimate accuracy but its capability to predict lane-change maneuvers.

Figs. 2 and 3 show the results obtained by the proposed IMM-based method in two cases of GPS signal availability. In each of these figures, the upper images show the model probabilities for the CL and KL maneuver states. As we can appreciate at first glance, the value of the CL state probability is much higher when lane-change actions are performed around time values of 5 and 9 s. In the bottom images of these figures, it can be seen how position and heading error values increase during these intervals. This time, the IMM noise estimates more realistically represent those errors (2σ envelopes for position and heading). The convenience of the proposed IMM method for a more accurate noise estimate anytime is clear.

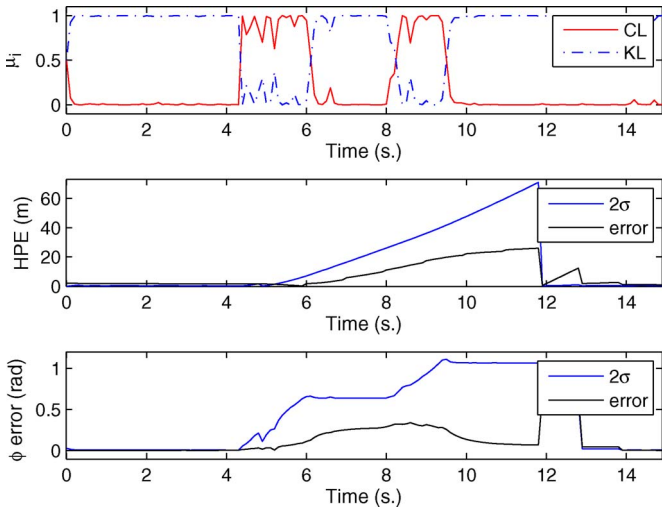

Fig. 3. Test with simulated GPS outage of 5 s (6–11) during a straight stretch. (Top) model probabilities of the CL (solid red) and KL (dash dotted blue) maneuver states. (Middle and bottom) Horizontal position and heading errors (solid black), and their corresponding 2σ envelopes (solid blue).

By means of reference measurements, we established manually the time at which the lane change started. Let us now analyze in detail the behavior of the system in the cases presented in this paper. According to the value of the angular acceleration obtained from reference measurements, the first lane change lasts from 4.2 to 5.9 s. After that, the vehicle still performs a smooth lateral movement until the instant 6.6 s. After that, from 6.7 to 7.8 s, the vehicle travels along the left lane. At 8 s, the vehicle starts another lane change but this time to the right lane, like in a common overtaking maneuver. This maneuver will last until the instant 9.3 s. After that, the vehicle still travels in the right lane until the end of the test.

Attending to the top graph of Fig. 2, the IMM outcomes for this maneuvering case can be observed. The probability of KL remains close to 1 until the instant 4.4 s, where the first value for the probability of CL higher than KL appears, just 0.2 s after the maneuver begins, according to the assumed reference. The probability of the CL state will remain higher until the instant 6 s. The algorithm classifies the period between 6.1 and 6.6 s as a KL state, assuming that the changes are not significant enough to represent a lane change, which is correct, according to the real vehicle trajectory. The probability of KL clearly remains higher until the instant 8.1 s. At 8.3 s, only 0.3 s after the assumed truth, the second lane change is predicted. A CL state is recognized by the IMM until the instant 9.4 s. Higher values of KL since 9.5 s inform us of the KL maneuver state until the end of the test.

The following conclusions can be obtained from this test. Maneuver state changes are typically predicted by the proposed IMM method between 0.2 and 0.3 s, which is around five times faster than using DGPS and map matching algorithms, according to [21]. Nevertheless, the filter phase shift provokes an inherent delay in the algorithm response.

Finally, observing Fig. 3, we can appreciate the consistency of the proposed method in the case of a GPS gap. As can be seen, the system performs well with GPS period outages of 5 s, which is a safe maximum value in highway scenarios. The use of inertial measurements supplies not only fast dynamic detection and maneuver prediction but also uninterrupted navigation in the absence of a GPS signal.

These tests previously discussed were performed in road segments with very low curvature values. Despite the fact that these low values correspond to most of the road segments in highway scenarios, it was found that in cases of more curved trajectories, the results obtained were poor, encouraging the use of road shape data in the filter.

TABLE II
POSITION AND HEADING ERRORS OF MODEL-SET B FILTERS

	KEEP LANE		CHANGE LANE		IMM	
Var.	rms	emax	rms	emax	rms	emax
Pos. (m)	0.63	1.80	0.54	1.73	0.52	1.78
Head. (rad)	0.10	0.31	0.04	0.16	0.04	0.15

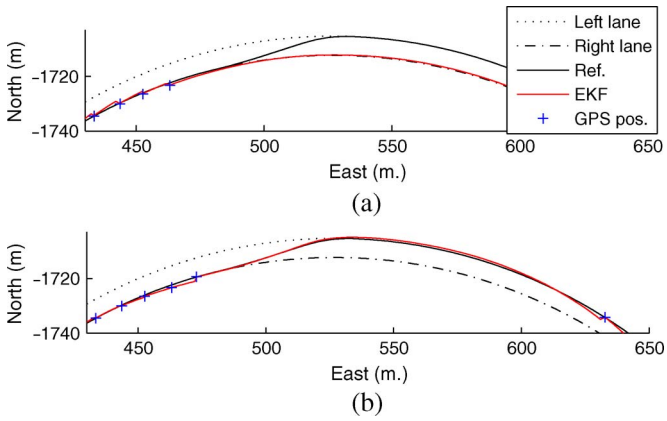

Fig. 4. Stretch of the N30 circuit with (a) the KL model and (b) the CL model. Right lane (dash-dotted black line), left lane (dotted black lane), Ground truth (solid black), EKF model trajectory (solid red), and GPS points (blue +). A GPS mask of 15 s is assumed.

C. Results With Model-Set B

To test its performance, model-set B has been evaluated by using the same data sets presented in Section IV-B (obtaining similar results) along with the circuit N30 presented in Section III-B3. The latter is analyzed in this section.

Table II shows the performance of this IMM implementation along the circuit N30. As can be seen, the error values for positioning and heading that are obtained in this test by the three filters under consideration are quite low. The CL values are smaller probably due to the number of lane changes performed by the car during the test. As in the previously analyzed model set, the IMM values are slightly lower than in the CL case.

Fig. 4 shows the performance of the KL and CL individual filters in the same stretch of the circuit N30. In both cases, the GPS signal has been masked to more easily appreciate their differences. Unlike the CL case, in the KL filter, the trajectory of the vehicle is assumed to meet the shape of the current road lane. Wherever this assumption is fulfilled by the dynamic conditions of the vehicle, the KL filter is selected by the IMM-based algorithm as the best model estimator due to its more restrictive noise considerations. In those cases where the vehicle dynamics does not comply the curvature features of the current road lane, the probability of the KL model diminishes, and the CL model arises, notifying a lane change. Fig. 5 shows both the model probabilities and the error estimates during the same road stretch. According to the literature, a lane change has been carried out when the four wheels of the vehicle have crossed the lane that separates two lanes. In the stretch presented, the CL model becomes higher than the KL model in the instant 3 s, which is only 0.2 s after the maneuver began and 1.4 s before crossing the lane line. The analysis of noise estimate values in this case is similar to the case realized in Section IV-B.

The mean value of the radius of curvature along this stretch of the road is 512.28 m. The curvature values, road shape, and GPS visibility conditions make this circuit very appropriate for testing the prediction algorithm. In the same way as in the previously analyzed model set, the influence of typical GPS outages in highways on the lane-change

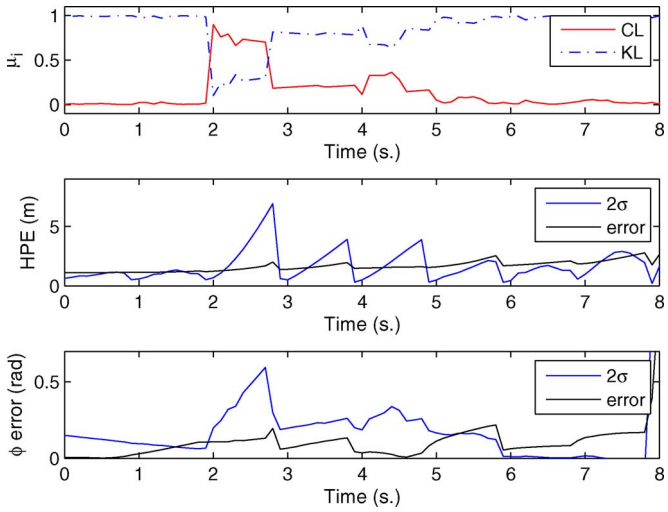

Fig. 5. Test with uninterrupted GPS coverage during a curved stretch. (Top) Model probabilities of the CL (solid red) and KL (dash dotted blue) maneuver states. (Middle and bottom) Horizontal position and heading errors (solid black), and their corresponding 2σ envelopes (solid blue).

TABLE III
TIME OF RESPONSE t_r AND TIME OF PREDICTION t_p OBTAINED IN THE EXPERIMENTS BY MODEL-SETS A AND B

	Model-set A	Model-set B
$t_r(s)$	0.3–0.4	0.3
$t_p(s)$	1.0–1.5	1.0–1.4

prediction can be neglected, having obtained similar results in tests performed with GPS masks of 2, 3, and 5 s.

Table III summarizes the values of time of response t_r and time of prediction t_p that are achieved by both model sets in our experiments. t_r represents the delay between the manual labeling and the filter response, whereas t_p stands for the difference between the instant when the vehicle fully crosses the lane line (which is accepted to be the actual moment when a vehicle completes a lane change) and the instant at which the maneuver is predicted by the algorithm. Model-set B, which was shown to also behave well in the case of road stretches of high curvature, presents t_p values of between 1 and 1.4 s, which can be considered to be useful for collision-avoidance applications.

V. CONCLUSION

The performance of an IMM-based algorithm for predicting lane changes in highways has been presented in this paper. A number of model sets were tested in real road circuits with different shapes. In those cases in which the road curvature is null or very low, model-set A, which is presented in Section IV-B, has been found to be suitable. However, its poor results on more curved trajectories encourage the use of road shape data in the prediction process. An algorithm to estimate the road curvature from UTM positions was applied and its value provided as input datum to the filter in model-set B (see Section IV-C). By estimating the vehicle and the road trajectories, model-set B achieves good results not only in straight road stretches but under challenging conditions of different curvature values and GPS blockages as well. The algorithm presented in this paper has been found to be useful for predicting lane changes with very short latency times.

Following the low-cost requirements, the sensor unit of the vehicle consists of a low-cost GPS receiver, a MEMS-based IMU (in which only one accelerometer and one gyro were used in the tests), and the odometry of the vehicle.

REFERENCES

[1] NHTSA Research and Development, *Evaluation of Lane Change Collision Avoidance Systems Using the National Advanced Driving Simulator*, 2002. [Online]. Available: http://www-nrd.nhtsa.dot.gov/departments/nrd-01/summaries/CAS_LaneChg.html
[2] J. C. McCall, D. P. Wipf, M. M. Trivedi, and B. D. Rao, "Lane change intent analysis using robust operators and sparse Bayesian learning," *IEEE Trans. Intell. Transp. Syst.*, vol. 8, no. 3, pp. 431–440, Sep. 2007.
[3] E. Mazor, A. Averbuch, Y. Bar-Shalom, and J. Dayan, "Interacting multiple model methods in target tracking: A survey," *IEEE Trans. Aerosp. Electron. Syst.*, vol. 34, no. 1, pp. 103–123, Jan. 1998.
[4] L. A. Johnston and V. Krishnamurthy, "An improvement to the interacting multiple model (IMM) algorithm," *IEEE Trans. Signal Process.*, vol. 49, no. 12, pp. 2909–2923, Dec. 2001.
[5] Y. Bar-Shalom and X. R. Li, *Multitarget–Multisensor Tracking: Principles and Techniques*. Storrs, CT: YBS, 1995.
[6] R. Toledo, M. Zamora, and A. Skarmeta, "IMM based maneuver detection and navigation for road vehicles with low cost GPS/IMU," in *Proc. IEEE Intell. Veh. Symp.*, Istanbul, Turkey, 2007, pp. 239–244.
[7] R. Toledo, M. Zamora, and A. Skarmeta, "Multiple model based lane change prediction for road vehicles with low cost GPS/IMU," in *Proc. IEEE ITSC*, Seattle, WA, 2007, pp. 473–478.
[8] R. Toledo, M. Zamora, B. Ubeda, and A. Skarmeta, "High-integrity IMM-EKF-based road vehicle navigation with low-cost GPS/SBAS/INS," *IEEE Trans. Intell. Transp. Syst.*, vol. 8, no. 3, pp. 491–511, Sep. 2007.
[9] Swedish Nat. Road Admin (Vägverket), "Vägutformning 94 vers. S-2," Tech. Rep., Borlänge, Sweden, 1994.
[10] S. Blackman and R. Popoli, *Design and Analysis of Modern Tracking Systems*. Norwood, MA: Artech House, 1999.
[11] A. Eidehall, "Tracking and threat assessment for automotive collision avoidance," Ph.D. dissertation, Linköping Univ., Linköping, Sweden, 2007.
[12] M. A. Zamora, D. Betaille, F. Peyret, and C. Joly, "Comparative study of extended Kalman filter, linearised Kalman filter and particle filter applied to low-cost GPS-based hybrid positioning system for land vehicles," *Int. J. Intell. Inform. Database Syst.*, vol. 2, no. 2, pp. 149–166, May 2008.
[13] D. Huang and H. Leung, "EM-IMM based land-vehicle navigation with GPS/INS," in *Proc. IEEE ITSC*, Washington, DC, 2004, pp. 624–629.
[14] C. Barrios, H. Himberg, Y. Motai, and A. Sadek, "Multiple model framework of adaptive extended Kalman filtering for predicting vehicle location," in *Proc. IEEE ITSC*, Toronto, ON, Canada, 2006, pp. 1053–1059.
[15] C. Hoffmann and T. Dang, "Cheap joint probabilistic data association filters in an interacting multiple model design," in *Proc. IEEE MFI*, Heidelberg, Germany, 2006, pp. 197–202.
[16] M. Jabbour, P. Bonnifait, and V. Cherfaoui, "Management of landmarks in a GIS for an enhanced localisation in urban areas," in *Proc. IEEE Intell. Veh. Symp.*, Tokyo, Japan, 2006, pp. 50–57.
[17] E. D. Dickmanns and A. Zapp, "A curvature-based scheme for improving road vehicle guidance by computer vision," in *Proc. SPIE Conf. Mobile Robots*, 1986, pp. 161–168.
[18] Z. Zomotor and U. Franke, "Sensor fusion for improved vision based lane recognition and object tracking with range-finders," in *Proc. IEEE ITSC*, 2001, pp. 595–600.
[19] S. Vacek, S. Bergmann, U. Mohr, and R. Dillmann, "Fusing image features and navigation system data for augmenting guiding information displays," in *Proc. IEEE MFI*, Heidelberg, Germany, 2006, pp. 323–328.
[20] J. Melo, A. Naftel, A. Bernardino, and J. Santos-Victor, "Detection and classification of highway lanes using vehicle motion trajectories," *IEEE Trans. Intell. Transp. Syst.*, vol. 7, no. 2, pp. 188–200, Jun. 2006.
[21] H.-S. Tan and J. Huang, "DGPS-based vehicle-to-vehicle cooperative collision warning: Engineering feasibility viewpoints," *IEEE Trans. Intell. Transp. Syst.*, vol. 7, no. 4, pp. 415–428, Dec. 2006.
[22] S. Rogers and W. Zhang, "Development and evaluation of a curve rollover warning system for trucks," in *Proc. IEEE Intell. Veh. Symp.*, 2003, pp. 294–297.
[23] S. Schroedl, K. Wagstaff, S. Rogers, P. Langley, and C. Wilson, "Mining GPS traces for map refinement," *Data Mining Knowl. Discov.*, vol. 9, no. 1, pp. 59–87, Jul. 2004.
[24] Z. Kim, "Realtime lane tracking of curved local road," in *Proc. IEEE ITSC*, 2006, pp. 1149–1155.
[25] K. Baass and J. Vouland, "Détermination de L'Aligment routier À partir de Traces GPS," in *Proc. Congrès Annuel de L'ATC*, Calgary, AB, Canada, 2005.